Origin of the Unique Stability of Condensed-Phase Hg_2^{2+}. An ab Initio Investigation of M^I and M^{II} Species (M = Zn, Cd, Hg)

Martin Kaupp* and Hans Georg von Schnering

Max-Planck-Institut für Festkörperforschung, Heisenbergstrasse 1, 70569 Stuttgart, Germany

Received November 4, 1993[⊗]

The stability of the Hg_2^{2+} cation and related species is due to differential aggregation/solvation effects in the condensed phase. These are strongly modified by relativistic effects. Thus, relativity is responsible for the existence of Hg–Hg-bonded species, but only in the condensed phase, and the stability is not due to the relativistic strengthening of the metal–metal bond itself, as suggested earlier. Ab initio pseudopotential calculations at theoretical levels higher than previously reported show that relativistic effects clearly shift the equilibrium $Hg_2X_2(g) \rightleftharpoons HgX_2(g) + Hg(g)$ (X = F, Cl, H) to the right and not to the left. There is a considerably greater chance to find the corresponding Zn–Zn- or Cd–Cd-bonded species in the gas phase! In the condensed phase, differential aggregation or solvation effects favor the Hg_n^{2+} cations: (a) The shift of the equilibrium to the right by the aggregation energy of the elemental metal is less pronounced for M = Hg than for M = Zn and Cd, very likely due to relativity. (b) The relativistic reduction of aggregation or solvation energies is larger for HgX_2 species than for the corresponding Hg_2X_2 compounds. This is shown by calculations on molecular model systems, $MCl_2{\cdot}H_2O$, $M_2Cl_2{\cdot}H_2O$, $(MF_2)_2$, and $(M_2F_2)_2$, and by periodic Hartree–Fock calculations on solid Hg_2F_2 and HgF_2.

I. Introduction

One of the most remarkable features of mercury chemistry is the existence of Hg–Hg-bonded cationic species in the condensed phase. In particular, the Hg_2^{2+} cation is found in many solid-state compounds, in melts, and in solution.[1-4] Additionally, larger cationic species like Hg_3^{2+} and Hg_4^{2+} (in $Hg_n(AsF_6)_2$, $n = 3,4$[5]) as well as the infinite-linear-chain species $Hg_{3-\delta}EF_6$ (E = As, Sb, Nb, Ta)[6] are known. In contrast, M–M-bonded cations for the lighter homologues of Zn and Cd are rare. Only one structurally characterized compound containing the Cd_2^{2+} cation ($Cd_2(AlCl_4)_2$) is known.[7] The evidence for the existence of the Zn_2^{2+} cation largely rests on spectroscopic data for $Zn/ZnCl_2$ glasses.[8]

Relativistic effects are well-known to influence the chemistry of heavy elements like mercury significantly.[9-16] It has been suggested that the exceptional stability of Hg_2X_2 species (e.g. X = F, Cl) is related to the relativistic stabilization of the Hg–Hg bond,[9a,b,10b,12b,13b,c,14] in analogy to the Au–Au bond in the gold dimer. However, in spite of a slight relativistic stabilization of the Hg–Hg bond, the available computational data indicate that the (gas-phase) equilibrium

$$Hg_2X_2 \rightleftharpoons HgX_2 + Hg \qquad (1)$$

is shifted to the right and not to the left by relativity.[14] As this equilibrium determines the thermochemial stability of Hg_2X_2 in the gas phase, an explanation for the stability of $(Hg^I)_2$ species based on the relativistic strengthening of the Hg–Hg bond is not in agreement with the computational evidence (the free Hg_2^{2+} ion is metastable and even slightly destabilized by relativity[13d]). This suggests that intrinsic condensed-phase interactions are responsible for the stability of Hg–Hg-bonded cations.

The cited calculations have been performed at the Hartree–Fock (HF) and MP2 ab initio levels and at the local density functional (LDA) theory level.[14] To be certain that a "molecular" explanation may indeed be ruled out, we performed more accurate quadratic configuration interaction (QCISD and QCISD(T)[17])

* Author to whom correspondence should be addressed. Temporary address from Nov 1993 through Oct 1994: Département de Chimie, Université de Montréal, C.P. 6128, Succ. A, Montréal, Québec H3C 3J7, Canada.

⊗ Abstract published in *Advance ACS Abstracts,* July 15, 1994.

(1) (a) Cotton, F. A.; Wilkinson, G. *Advanced Inorganic Chemistry*, 5th ed.; Wiley: New York, 1988. (b) Greenwood, N. N.; Earnshaw, A. *Chemistry of the Elements*; Pergman Press: Oxford, U.K., 1984. (c) Wells, A. F. *Structural Inorganic Chemistry*, 5th ed.; Clarendon Press: Oxford, U.K., 1984.

(2) Brodersen, K.; Hummel, H.-U. In *Comprehensive Coordination Chemistry*; Wilkinson, G., Ed.; Pergaman Press: Oxford, U.K., 1987; Vol. 5.

(3) Aylett, B. J. In *Comprehensive Inorganic Chemistry*; Trotman-Dickenson, Ed.; Pergamon Press: Oxford, U.K., 1973; Vol. 3.

(4) For further reviews on mercury coordination chemistry see, e.g.: Grdenic, D. *Q. Rev.* **1965**, *19*, 303. Dean, P. A. W. *Prog. Inorg. Chem.* **1978**, *24*, 109. Grdenic, D. In *Structural Studies of Molecular Biological Interest*; Dodson, G., Glusker, J. P., Sayre, D., Eds.; Clarendon Press: Oxford, U.K., 1981. Levason, W.; McAuliffe, C. A. In *The Chemistry of Mercury*; McAuliffe, C. A., Ed.; Macmillan: London, 1977. Brodersen, K. *Comments Inorg. Chem.* **1981**, *1*, 207.

(5) (a) Davies, C. G.; Dean, P. A. W.; Gillespie, R. J.; Ummat, P. K. *J. Chem. Soc. D* **1971**, 782. (b) Cutforth, B. D.; Gillespie, R. J.; Ireland, P. R. *J. Chem. Soc., Chem. Commun.* **1973**, 723. Cutforth, B. D.; Gillespie, R. J.; Ireland, P. R.; Sawyer, J. F.; Ummat, P. K. *Inorg. Chem.* **1983**, *22*, 1344.

(6) Cutforth, B. D.; Davies, C. G.; Dean, P. A. W.; Gillespie, R. J.; Ireland, P. R.; Ummat, P. K. *Inorg. Chem.* **1973**, *12*, 1343. Gillespie, R. J.; Ummat, P. K. *J. Chem. Soc. D* **1971**, 1168. Tun, Z.; Brown, I. D.; Ummat, P. K. *Acta Crystallogr. Sect., C* **1984**, *40*, 1301.

(7) Faggiani, R.; Gillespie, R. J.; Vekris, J. E. *J. Chem. Soc., Chem. Commun.* **1986**, 517. Staffel, T.; Meyer, G. *Z. Allg. Anorg. Chem.* **1987**, *548*, 45.

(8) Kerridge, D. H.; Tariq, S. A. *J. Chem. Soc. A* **1967**, 1122.

(9) (a) Pyykkö, P. *Chem. Rev.* **1988**, *88*, 563. (b) Pyykkö, P. *Adv. Quantum Chem.* **1978**, *11*, 353. (c) Pyykkö, P.; Desclaux, J. P. *Acc. Chem. Res.* **1979**, *12*, 276.

(10) (a) Pitzer, K. S. *Acc. Chem. Res.* **1979**, *12*, 271. (b) Christiansen, P. A.; Ermler, W. C.; Pitzer, K. S. *Annu. Rev. Phys. Chem.* **1985**, *36*, 407.

(11) (a) Norrby, L. J. *J. Chem. Educ.* **1991**, *60*, 110. (b) Moriarty, J. A. *Phys. Lett. A* **1988**, *131*, 41.

(12) (a) Schwarz, W. H. E. *Phys. Scr.* **1987**, *36*, 403. (b) Schwarz, W. H. E. In *Theoretical Models of Chemical Bonding*; Maksic, B., Ed.; Springer: Berlin, 1990; Vol. 2, p 593.

(13) (a) Strömberg, D.; Gropen, O.; Wahlgren, U. *Chem. Phys.* **1989**, *133*, 207. (b) Ziegler, T.; Snijders, J. G.; Baerends, E. J. *J. Chem. Phys.* **1981**, *74*, 1271. (c) Neisler, R. P.; Pitzer, K. S. *J. Phys. Chem.* **1987**, *91*, 1084. (d) Strömberg, D.; Wahlgren, U. *Chem. Phys. Lett.* **1990**, *169*, 109. (e) Durand, G.; Spiegelmann, F.; Bernier, A. *J. Phys. B* **1987**, *20*, 1161.

(14) Schwerdtfeger, P.; Boyd, P. D. W.; Brienne, S.; McFeaters, J.; Dolg, M.; Liao, M.-S.; Schwarz, W. H. E. *Inorg. Chim. Acta* **1993**, *213*, 233.

(15) (a) Kaupp, M.; von Schnering, H. G. *Angew. Chem.* **1993**, *105*, 952; *Angew. Chem., Int. Ed. Engl.* **1993**, *32*, 861. (b) Kaupp, M.; Dolg, M.; Stoll, H.; von Schnering, H. G. *Inorg. Chem.* **1994**, *33*, 2122.

(16) (a) Kaupp, M.; von Schnering, H. G. *Inorg. Chem.* **1994**, *33*, 2555. (b) Kaupp, M.; von Schnering, H. G. *Inorg. Chem.*, in press.

(17) See, e.g.: Pople, J. A.; Head-Gordon, M.; Raghavachari, K. *J. Chem. Phys.* **1987**, *87*, 5968. Paldus, J.; Cizek, J.; Jeziorski, B. *J. Chem. Phys.* **1989**, *90*, 4356; **1990**, *93*, 1485. Raghavachari, K.; Head-Gordon, M.; Pople, J. A. *J. Chem. Phys.* **1990**, *93*, 1486.

0020-1669/94/1333-4179$04.50/0

pseudopotential calculations on M_2X_2 (M = Zn, Cd, Hg; X = F, Cl, H), using extended valence basis sets. Compounds of the lighter group 12 metals Zn and Cd were studied to make a definite comparison of the gas-phase thermochemical stability of the group 12 M_2X_2 species. It turns out that the Zn_2X_2 and Cd_2X_2 species are actually more stable toward the gas-phase disproportionation (1) than the corresponding mercury species.

Recently, we showed that relativity significantly reduces the electrostatic interactions between HgX_2 molecules.[16] Following this line, we provide calculations on molecular model systems and on the crystalline mercury fluorides that compare the solvations and aggregations of M_2X_2 and MX_2 species (M = Zn Cd, Hg). Our results show that the relativistic reduction of HgX_2 aggregation (solvation) energies and the less pronounced relativistic reduction of Hg_2X_2 aggregation (solvation) energies, as well as the relativistically reduced[9,11] aggregation energy for elemental mercury, contribute to the unique stability of Hg_2^{2+} in the condensed phase.

The setup of this paper is as follows: Section II describes the computational methods employed. Sections III–V are concerned with the gas-phase structural and stability results and with establishing the accuracy of our calculations. Sections VI–VIII evaluate the influence of various condensed-phase interactions. A summary is given in section IX.

II. Computational Methods

A. Molecular Calculations. We used the same quasirelativistic 20-valence-electron pseudopotentials for Zn,[18] Cd,[19] and Hg[19] as in our recent studies of group 12 chemistry.[15,16] Comparative calculations with a nonrelativistic Hg pseudopotential[19] provide information on the influence of relativistic effects on molecular properties of the mercury compounds. For F and Cl, we employed 7-valence-electron pseudopotentials.[20]

We made use of the two different basis set contraction schemes described in our recent study of group 12 M^{IV} fluorides:[15b] Segmented (8s7p6d)/[6s5p3d] valence basis sets published with the Zn, Cd, and Hg pseudopotentials[18,19] were used with segmented (5s5p1d)/[3s3p1d] valence basis sets for F and Cl[21] and a (4s1p)/[2s1p] basis for hydrogen.[22] This basis set combination will be designated basis A. The addition of one metal f function[15b] leads to basis **B**. This basis set level should be comparable to that used by Schwerdtfeger et al. on Hg_2X_2.[14] Our large-scale QCISD and QCISD(T)[17] calculations employed generally contracted (ANO[23]) metal (8s7p6d2f)/[4s3p3d2f] valence basis sets,[15b] halogen (7s7p3d1f)/[3s3p3d1f] ANO valence bases,[15b] and a (7s2p)/[3s2p] hydrogen basis.[24]

We follow the conventional notation for the computational levels.[25] The structures of linear M_2X_2, MX_2, and MX were optimized at the HF/basis A and MP2/basis A levels. Subsequently, the M–M distances in M_2X_2 were optimized at the MP2/basis **B** level and for M = Hg at the ANO–MP2 and ANO–QCISD levels, keeping the M–X distances at their MP2/basis A values. Final ANO–QCISD(T) energy calculations employed the MP2/basis B M–M distances and MP2/basis A M–X distances.

The complexes $M_2Cl_2{\cdot}H_2O$ and $MCl_2{\cdot}H_2O$, which serve to model the solvation of the chlorides, were optimized at the MP2 and HF levels with basis A on the metals, a 6-valence-electron pseudopotential for oxygen,[20] (4s4p1d)/[2s2p1d] valence basis sets for O[20] and Cl,[21] and a DZ hydrogen basis[22] (i.e., the diffuse sp set on Cl and the p function on H were removed from basis A). The dimers $(M_2F_2)_2$ and $(MF_2)_2$ were optimized at the HF/basis A level with subsequent MP2/basis A single-point calculations.

In MP2 and QCI calculations, all of the electrons outside the pseudopotential cores (including the metal $(n-1)$ shells) were included in the active space. Calculations of open-shell fragments (e.g. the MX molecules) were based on UHF reference wave functions. Reaction energies were not corrected for zero-point vibrational energies. The calculations employed the Gaussian92[26] and MOLPRO[27] program systems.

B. Periodic Hartree–Fock Calculations on Crystalline Hg_2F_2. Hartree–Fock calculations on bulk Hg_2F_2 were carried out using the Crystal 92 program.[28] We employed the same computational parameters as for our recent investigations of solid HgF_2 and CdF_2.[16b] Briefly, our calculations employed the same mercury pseudopotentials (both quasirelativistic and nonrelativistic[19]) and also the same F pseudopotential[20] as our molecular calculations (cf. above). The construction of the 4s4p2d (Hg) and 2s2p (F) valence basis sets will be described elsewhere.[16b]

Hg_2F_2 is known to crystallize in space group $I4/mmm$,[29] and our calculations were restricted to this symmetry. Thus, four independent structural parameters had to be optimized: the lattice constants a and c, as well as the positional parameters z(Hg) and z(F). This was done by pointwise variation, with both the quasirelativistic and the nonrelativistic mercury pseudopotentials.

Basis set superposition error (BSSE) contributions to the sublimation energies were estimated using the counterpoise correction,[30] both for the solid and for the monomeric molecule (at the same basis set level). For the crystal, only the basis functions for the nearest and next-nearest neighbors (fluorine atoms for Hg_2^{2+} and mercury atoms for F^-) were considered.

Table 1. Hg–Hg Distances (Å) in Hg_2X_2 (X = H, F, Cl) at Different Computational Levels

X	HF/ basis A	MP2/ basis A	MP2/ basis B[a]	ANO–MP2[a]	ANO–QCISD[a]
F	2.610 (2.925)[b]	2.568 (2.845)[b]	2.492 (2.738)[b]	2.541	2.563
Cl	2.641 (2.946)[b]	2.590 (2.860)[b]	2.518 (2.755)[b]	2.571	2.589
H	2.717 (3.003)[b]	2.667 (2.915)[b]	2.594 (2.806)[b]	2.602	2.645

[a] Hg–X distances kept fixed at MP2/basis A optimized values. [b] Nonrelativistic Hg pseudopotential results in parentheses.

Table 2. HF and MP2 Optimized M–M Distances (Å) in M_2X_2 (M = Zn, Cd; X = F, Cl, H)

species	HF	MP2/basis A	MP2/basis B[a]
Zn_2F_2	2.404	2.311	2.293
Zn_2Cl_2	2.427	2.332	2.310
Zn_2H_2	2.500	2.402	2.380
Cd_2F_2	2.695	2.615	2.557
Cd_2Cl_2	2.719	2.632	2.572
Cd_2H_2	2.787	2.695	2.637

[a] MP2/basis B optimizations of the M–M distance with fixed MP2/basis A M–X distances.

III. Bond Distances for M_2X_2

Before going into the thermochemical details, it is worthwhile to compare the M–M distances obtained at various computational levels. Table 1 provides the results for the Hg_2X_2 species. The HF/basis A and MP2/basis B calculations correspond closely to the HF and MP2 methods used by Schwerdtfeger et al.,[14] and the data do indeed agree excellently. Our best ANO–QCISD

(18) Dolg, M.; Wedig, U.; Stoll, H.; Preuss, H. *J. Chem. Phys.* **1987**, *86*, 866.
(19) Andrae, D.; Häussermann, U.; Dolg, M.; Stoll, H.; Preuss, H. *Theor. Chim. Acta* **1990**, *77*, 123.
(20) Bergner, A.; Dolg, M.; Küchle, W.; Stoll, H.; Preuss, H. *Mol. Phys.* **1993**, *80*, 1431.
(21) (a) Kaupp, M.; Schleyer, P. v. R.; Stoll, H.; Preuss, H. *J. Am. Chem. Soc.* **1991**, *113*, 6012–6020. (b) Huzinaga, S., Ed. *Gaussian Basis Sets for Molecular Calculations*; Elsevier: New York, 1984.
(22) Dunning, T. H.; Hay, P. J. In *Methods of Electronic Structure Theory, Modern Theoretical Chemistry*; Schaefer, H. F., III, Ed.; Plenum Press: New York, 1977; Vol. 3.
(23) Almlöf, J.; Taylor, P. R. *J. Chem. Phys.* **1987**, *86*, 4070.
(24) Dunning, T. H. *J. Chem. Phys.* **1989**, *90*, 1007.
(25) Explanations of standard levels of ab initio MO theory, such as the Hartree–Fock (HF) and MP*n* methods, may be found, e.g., in: Hehre, W. J.; Radom, L.; Schleyer, P. v. R.; Pople, J. A. *Ab Initio Molecular Orbital Theory*; Wiley: New York, 1986.
(26) Frisch, M. J.; Trucks, G. W.; Head-Gordon, M.; Gill, P. M. W.; Wong, M. W.; Foresman, J. B.; Johnson, B. G.; Schlegel, H. B.; Robb, M. A.; Replogle, E. S.; Gomperts, R.; Andres, J. L.; Raghavachari, K.; Binkley, J. S.; Gonzalez, C.; Martin, R. L.; Fox, D. I.; DeFrees, D. J.; Baker, J.; Stewart, J. P.; Pople, J. A. *Gaussian 92*, Revision A; Gaussian, Inc.: Pittsburgh, PA, 1992.
(27) Program system MOLPRO written by H. J. Werner, and P. J. Knowles, with contributions by J. Almlöf, R. Amos, S. Elbert, C. Hampel, W. Meyer, K. Peterson, R. Pitzer, and A. Stone.
(28) Crystal 92 program by R. Dovesi, V. R. Saunders, C. Roetti, et al., 1992. For a general description, cf.: Pisani, C.; Dovesi, R.; Roetti, C. *Hartree-Fock ab Initio Treatment of Crystalline Systems, Lecture Notes in Chemistry*; Springer: Berlin, 1988.
(29) Dorm, E. *J. Chem. Soc., Chem. Commun.* **1970**, 466.
(30) Boys, S. F.; Bernardi, F. *Mol. Phys.* **1970**, *19*, 553.

Table 3. M–X Distances (Å) in M_2X_2, MX_2, and MX

		M_2X_2		MX_2		MX	
M	X	HF/basis A	MP2/basis A	HF/basis A	MP2/basis A	HF/basis A	MP2/basis A
Zn	F	1.776	1.773	1.743	1.741	1.794	1.794
Cd	F	1.983	1.986	1.949	1.959	2.008	2.016
Hg	F	2.009 (2.097)[a]	2.010 (2.103)[a]	1.953 (2.067)[a]	1.965 (2.079)[a]	2.060 (2.118)[a]	2.060 (2.129)[a]
Zn	Cl	2.155	2.122	2.116	2.089	2.183	2.152
Cd	Cl	2.359	2.328	2.314	2.292	2.395	2.369
Hg	Cl	2.370 (2.483)[a]	2.339 (2.455)[a]	2.313 (2.441)[a]	2.293 (2.421)[a]	2.441 (2.516)[a]	2.408 (2.492)[a]
Zn	H	1.588	1.540	1.558	1.509	1.616	1.565
Cd	H	1.744	1.706	1.708	1.672	1.780	1.739
Hg	H	1.697 (1.858)[a]	1.658 (1.818)[a]	1.664 (1.819)[a]	1.632 (1.782)[a]	1.778 (1.889)[a]	1.711 (1.848)[a]

[a] Nonrelativistic Hg pseudopotential results in parentheses.

values (last column) should be taken as a reference to judge these more approximate methods.

The Hg–Hg distances are shortest at the MP2/basis B level. Improvement of the valence basis sets (ANO–MP2) expands the bond lengths by ca. 0.05 Å for X = F and Cl. This suggests that basis set superposition errors (BSSE) due to the limited halogen valence bases at the MP2/basis B level exaggerate the bond contraction by electron correlation (compare HF results, first column). Moreover, the Hg–Hg bonds lengthen slightly (by ca. 0.02–0.04 Å) upon going from ANO–MP2 to ANO–QCISD. The MP2/basis A distances (no metal f function) agree quite closely with the best ANO–QCISD values, due to error compensation (this has been observed previously for Hg–X distances in HgX_2[15,16]). These distances are slightly larger (by ca. 0.04–0.08 Å) than most solid-state data for comparable systems,[2-4,29] except for very recent powder neutron diffraction data on Hg_2Cl_2 (r(Hg–Hg) = 2.5955 Å),[31] which are in essentially perfect agreement with our ANO–QCISD value (2.589 Å) for the molecule (also see section VIII.B and ref 14 for comparisons to experimental data).

HF and MP2 M–M distances for the zinc and cadmium species are shown in Table 2. As for the Hg species, correlation shortens the M–M distances (note that this contraction is smallest for the mercury species at the quasirelativistic pseudopotential level). The addition of a metal f function (MP2/basis B vs MP2/basis A) leads to a contraction for Cd_2X_2 similar to that for Hg_2X_2, but less so for Zn_2X_2. Assuming that the same compensation of basis set and MP2 errors is operative as for the Hg–Hg bond, the MP2/basis A values may serve as good estimates of higher-level results. This suggests that the Cd–Cd separations are somewhat larger than the corresponding Hg–Hg distances for a given X, due to the relativistic contraction of the Hg–Hg bonds (compare Table 1). Indeed, the experimental Cd–Cd distance in $Cd_2(AlCl_4)_2$ is ca. 2.57 Å,[7] slightly longer than Hg–Hg distances for comparable species (ca. 2.50 Å[2-4]). The calculated Zn–Zn distances are considerably shorter, in the range 2.3–2.4 Å.

Cd–X and Hg–X distances in M_2X_2, MX_2, and MX are quite similar for a given X, again due to the relativistic contraction of the Hg–X bonds (cf. Table 3). Notably, all M–X distances in MX_2 are slightly (ca. 0.03–0.05 Å) shorter than those in M_2X_2 for the same X, consistent with a larger destabilizing trans influence of the MX vs X substituents.[32] The longer M–X distances in the MX radicals (Table 3) may be ascribed to an even larger trans influence of the unpaired electron in these monovalent metal species. Alternatively, the differences in the M–X distances for MX_2 and MX may be explained by simple hybridization arguments.[33]

IV. M–M Binding Energies

Table 4 summarizes the energies calculated at various levels for the dissociation reaction $M_2X_2 \rightarrow 2MX$. Our highest-level (ANO–QCISD(T)) energies are given in the last column. Consistent with the above discussion of the M–M distances, the comparison of the MP2/basis B to the extended-basis ANO–MP2 energies for X = F and Cl reveals considerable BSSE for the former; i.e., the binding energies with the smaller halogen valence bases are too large by up to 16 kJ mol^{-1}. In addition, the MP2 method overestimates binding (by ca. 15–20 kJ mol^{-1} for M = Zn, by ca. 25–30 kJ mol^{-1} for M = Cd and nonrelativistic M = Hg, and by ca. 40–45 kJ mol^{-1} for relativistic M = Hg), as judged by comparison of the ANO–MP2 to the ANO–QCISD results. Finally, inclusion of triple substitutions (QCISD(T) vs QCISD calculations) increases the binding energies by ca. 5–10 kJ mol^{-1}. As a result, the MP2/basis B calculations overestimate the M–M binding energies for the halides (QCISD(T) values taken as a reference) by roughly 20–35 kJ mol^{-1} for M = Zn and Cd and by up to ca. 50 kJ mol^{-1} for M = Hg at the quasirelativistic pseudopotential level. This has a considerable effect on the disproportionation equilibrium (1) (cf. below). The agreement between MP2/basis B and ANO–QCI results is better for the hydrides than for the halides.

Table 4. M–M Binding Energies[a] (kJ mol^{-1}) for M_2X_2 at Various Computational Levels[b]

M	X	MP2/basis B	ANO–MP2	ANO–QCISD	ANO–QCISD(T)
Zn	F	278.9	273.8	257.4	263.1
Cd	F	266.1	250.5	224.7	233.9
Hg	F	327.4 (251.9)[c]	312.9 (252.2)[c]	270.8 (224.2)[c]	281.2 (233.3)[c]
Zn	Cl	276.2	268.9	251.3	256.5
Cd	Cl	263.1	251.8	220.9	228.0
Hg	Cl	309.5 (252.7)[c]	293.3 (248.1)[c]	248.9 (214.1)[c]	257.3 (222.3)[c]
Zn	H	250.9	260.9	242.2	247.4
Cd	H	245.1	252.4	225.4	232.0
Hg	H	268.2 (242.2)[c]	278.6 (258.5)[c]	250.6 (232.5)[c]	256.9 (238.7)[c]

[a] Energies for the reaction $M_2X_2 \rightarrow 2MX$. [b] Calculated with MP2/basis A optimized M–X distances (Table 3) and MP2/basis B optimized M–M distances (Tables 1 and 2). [c] Nonrelativistic Hg pseudopotential results in parentheses.

The relativistic increase of the Hg–Hg dissociation energies reported earlier[14] is apparent from the data in Table 4, regardless of the computational level employed. Thus, while the nonrelativistic pseudopotential results for Hg_2X_2 are quite similar to the data for the Cd–Cd bond, relativity strengthens the Hg–Hg bond (by up to ca. 50 kJ mol^{-1} for the fluoride). As a result, the trend in the M–M dissociation energies for a given X is generally Hg–Hg > Zn–Zn > Cd–Cd. However, while the QCI Cd–Cd binding energies are significantly smaller (by ca. 20–50 kJ mol^{-1}) than those for the other two metals, the Zn–Zn and Hg–Hg binding energies are not too different, particularly for X = Cl (Table 4). The reported increase of the M–M binding energies with increasing electronegativity of X[14] is confirmed by our calculations. However, note that the ANO–QCISD(T) Hg–Hg binding energies in Hg_2H_2 and in Hg_2Cl_2 are very similar, in contrast to

(31) Calos, N. J.; Kennard, C. H. L.; Davis, R. L. *Z. Kristallogr.* **1989**, *187*, 305.
(32) Reinhold, J.; Steinfeldt, N.; Schüler, M.; Steinborn, D. *J. Organomet. Chem.* **1992**, *425*, 1.
(33) For a discussion see, e.g.: Kutzelnigg, W. *Angew. Chem.* **1984**, *96*, 262; *Angew. Chem., Int. Ed. Engl.* **1984**, *23*, 272.

Table 5. Energies (kJ mol^{-1}) for the Gas-Phase Disproportionation Reaction $M_2X_2 \rightarrow MX_2 + M$ at Various Computational Levels[a]

M	X	MP2/basis B	ANO–MP2	ANO-QCISD	ANO–QCISD(T)
Zn	F	+80.8	+56.7	+37.0	+36.7
Cd	F	+87.6	+42.9	+27.6	+29.3
Hg	F	+53.5 (+90.0)[b]	+13.4 (+63.3)[b]	+5.6 (+48.9)[b]	+7.1 (+50.6)[b]
Zn	Cl	+72.4	+52.1	+30.7	+30.4
Cd	Cl	+74.4	+38.8	+21.8	+22.2
Hg	Cl	+37.5 (+79.1)[b]	+6.2 (+55.1)[b]	−8.6 (+32.7)[b]	−5.9 (+34.5)[b]
Zn	H	+5.8	−14.4	−30.7	−30.5
Cd	H	+6.6	−29.2	−38.7	−37.7
Hg	H	−40.0 (+13.9)[b]	−78.2 (−8.8)[b]	−86.8 (−16.7)[b]	−84.0 (−16.7)[b]

[a] Calculated with MP2/basis A optimized M–X distances (Table 3) and MP2/basis B optimized M–M distances (Tables 1 and 2). [b] Nonrelativistic Hg pseudopotential results in parentheses.

lower-level results (Table 4) which would suggest the bond in the chloride to be significantly stronger (also cf. ref 14).

V. Energies of Disproportionation ($M_2X_2(g) \rightleftharpoons MX_2(g) + M(g)$)

The energies for disproportionation into MX_2 and M^0 are more realistic measures of the gas-phase stability of the M_2X_2 species than those for the dissociation into MX radicals. Table 5 lists the energies of reaction 1 calculated at various theoretical levels. Due to the overestimate of the M–M binding energies (cf. above), the MP2 calculations also overestimate the stability of M_2X_2 toward disproportionation. This is particularly so with the relatively small halogen valence bases at the MP2/basis B level. The MP2 results reported by Schwerdtfeger et al.[14] are intermediate between the MP2/basis B and ANO–MP2 results in Table 5. The QCI calculations yield far smaller positive or more negative (for M_2H_2) reaction energies. In contrast to MP2 results, the QCI calculations suggest the (gas-phase) disproportionation $Hg_2Cl_2 \rightarrow HgCl_2 + Hg$ to be exothermic (vibrational corrections not included), in agreement with available experimental evidence.[34] Contributions from triple substitutions (QCISD(T) vs QCISD) to the reaction energies are generally small.

Regardless of the computational level employed, our calculations (Table 5) confirm[14] that relativity shifts equilibrium 1 to the right; i.e., it destabilizes the Hg_2X_2 species toward disproportionation by ca. 40–60 kJ mol^{-1}. This means a smaller positive reaction energy for X = F and a larger negative one for X = H. In the case of Hg_2Cl_2, relativity changes the reaction from endothermic to exothermic (at the QCI level). As a result, the Hg_2X_2 species are considerably less stable toward disproportionation than their Cd or particularly their Zn homologues (cf. Table 5): The order of stability is Zn > Cd > Hg. In the gas phase it should be easier to observe, e.g., Zn_2Cl_2 than Hg_2Cl_2. Thus, the gas-phase equilibrium (1) does not provide an explanation for the exceptional stability of the Hg_2^{2+} species in the condensed phase. Other possible explanations involving a comparison of energies of solvation or aggregation are investigated below.

VI. Contribution of the Metal Aggregation Energies

When the experimental heats of vaporization for Zn, Cd, and Hg (115.3, 99.9, and 61.3 kJ mol^{-1}, respectively[3]) are added to the ANO–QCISD(T) results (cf. Table 5) for the energies of the gas-phase reaction (1), the reactions all become strongly exothermic, even with the fluorides (Table 6). The reaction is now least exothermic for the mercury halides, due to the small aggregation energy of elemental mercury (which is probably due to relativity[9,11,35]). However, it is clear that considerable differential effects in the solvation or aggregation of the Hg_2X_2 and HgX_2 species must be involved to shift the reaction energies back to positive or at least only slightly negative values expected from the existence of the mercurous halides in the condensed phase. We will explore this in the following two sections.

Table 6. ANO–QCISD(T) Reaction Energies (kJ mol^{-1})[a] for Reaction 1 with Experimental Heats of Vaporization for the Elemental Metals[b] Added

	M		
X	Zn	Cd	Hg
F	−78.6	−70.6	−54.2
Cl	−84.9	−77.7	−67.2
H	−145.8	−137.6	−145.3

[a] Cf. Table 5. [b] From ref 3; see text.

Table 7. MP2(HF) Optimized Structural Parameters (Å, deg) for $MCl_2 \cdot H_2O$ Complexes[a]

M	M–Cl	M–O	Cl–M–Cl
Zn	2.121 (2.158)	2.133 (2.152)	151.2 (150.2)
Cd	2.327 (2.351)	2.370 (2.408)	159.2 (158.0)
Hg_{nr}[b]	2.454 (2.476)	2.474 (2.508)	160.8 (159.3)
Hg_{rel}[c]	2.314 (2.335)	2.587 (2.671)	170.5 (169.9)

[a] Cf. Figure 1. [b] Nonrelativistic Hg pseudopotential. [c] Quasirelativistic Hg pseudopotential.

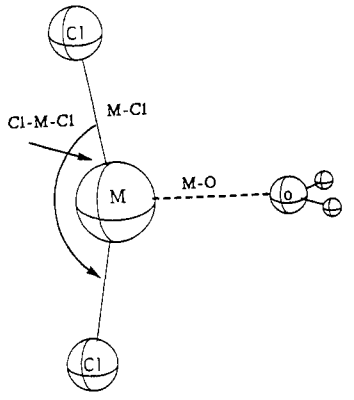

Figure 1. Internal coordinates for C_{2v} optimized structures of $MCl_2 \cdot H_2O$ used in Table 7.

VII. Influence of Solvation. Comparison of Model Complexes $MCl_2 \cdot H_2O$ and $M_2Cl_2 \cdot H_2O$ (M = Zn, Cd, Hg)

We have chosen the complexes of the chlorides MCl_2 and M_2Cl_2 with one water molecule to study the differential effects of the attachment of solvent molecules to the M^{II} and M^I species. Though admittedly crude models, these molecular complexes should provide a comparison of the trends down group 12 and particularly an estimate of relativistic effects on the solvation of the mercury species. The complexes $MCl_2 \cdot H_2O$ have been MP2-(HF) optimized in C_{2v} symmetry, and the major structural parameters obtained are listed in Table 7 (cf. Figure 1 for the definition of the internal coordinates). The $M_2Cl_2 \cdot H_2O$ complexes have been optimized in C_s symmetry (cf. Figure 2). The results are summarized in Table 8.

(34) Cf. e.g.: Roberts, H. L. *Adv. Inorg. Chem. Radiochem.* **1968**, *11*, 308.
(35) LDA band structure calculations on solid β-mercury (cf. ref 11b) suggest a decrease of ca. 180 kJ mol^{-1} in the cohesion energy, due to relativistic contributions. However, in view of the large discrepancies between calculated and experimental cohesive energies, this number may not be very reliable.

Table 8. MP2(HF) Optimized Structural Parameters (Å, deg) for $M_2Cl_2 \cdot H_2O$ Complexes[a]

M	M–M	M_1–Cl_1	M_2–Cl_2	M_1–O	Cl_1–M_1–M_2	Cl_2–M_2–M_1	O–M_1–M_2
Zn	2.338 (2.439)	2.176 (2.206)	2.132 (2.169)	2.204 (2.257)	152.1 (152.4)	179.3 (179.3)	114.9 (114.8)
Cd	2.627 (2.724)	2.378 (2.407)	2.339 (2.370)	2.426 (2.506)	158.9 (159.0)	179.5 (179.4)	114.2 (114.9)
Hg_{nr}[b]	2.859 (2.950)	2.507 (2.531)	2.463 (2.492)	2.535 (2.591)	159.1 (158.6)	179.4 (179.5)	118.3 (118.7)
Hg_{rel}[c]	2.589 (2.638)	2.372 (2.398)	2.344 (2.379)	2.652 (2.785)	171.5 (171.4)	179.3 (179.7)	104.3 (105.4)

[a] Cf. Figure 2. [b] Nonrelativistic Hg pseudopotential. [c] Quasirelativistic Hg pseudopotential.

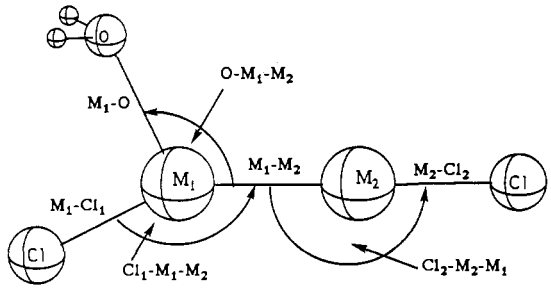

Figure 2. Internal coordinates for C_s optimized structures of $M_2Cl_2 \cdot H_2O$ used in Table 8.

Table 9. MP2(HF) Energies (kJ mol^{-1}) of Binding of a Water Molecule to MCl_2 and M_2Cl_2[a]

M	$MCl_2 \cdot H_2O$	$M_2Cl_2 \cdot H_2O$	M	$MCl_2 \cdot H_2O$	$M_2Cl_2 \cdot H_2O$
Zn	78.9 (71.4)	74.4 (55.8)	Hg_{nr}[b]	80.9 (69.3)	75.9 (57.1)
Cd	79.0 (66.3)	75.5 (55.7)	Hg_{rel}[c]	50.9 (40.0)	55.7 (39.7)

[a] Cf. Tables 7 and 8 for the corresponding MP2(HF) optimized structures. [b] Nonrelativistic Hg pseudopotential. [c] Quasirelativistic Hg pseudopotential.

The influence of relativity on the structure of $HgCl_2 \cdot H_2O$ is remarkable (Table 7): While the Hg–Cl bonds show the usual contraction,[9-16] the Hg–O bond is lengthened by 0.12 Å (0.26 Å) at MP2(HF). Thus, while the M–Cl and M–O bond lengths for the Zn and Cd complexes are similar, the Hg–Cl bond is much shorter than the Hg–O distance at the quasirelativistic pseudopotential level (in agreement with experimental evidence in solution[36]). The Cl–Hg–Cl angle is increased from ca. 160° (which would be similar to the results for M = Zn and Cd) to ca. 170° by relativity. Large relativistic effects on X–Hg–X bond angles have been computed previously for the HgX_2 dimers.[16a]

Similar structural effects of relativity occur for $Hg_2Cl_2 \cdot H_2O$ (Table 8): The Hg–Cl bonds contract, the Hg_1–O bond expands (by ca. 0.12 Å at MP2), and the Cl_1–M_1–Cl_2 angle increases by ca. 13°. Additionally, the O–Hg_1–Hg_2 angle decreases, consistent with a reduced Hg_1–OH_2 interaction (cf. below). As for the MCl_2 complexes, the resulting M–O and M–Cl distances are similar for M = Zn and Cd but quite different for M = Hg. The M–O bonds in the $HgCl_2 \cdot H_2O$ and $Hg_2Cl_2 \cdot H_2O$ complexes provide nice examples for relativistic bond length expansion (this behavior is much rarer than bond contraction[9a]). Note that the Hg–O bonds in both mercury complexes contract more in going from HF to MP2 than the M–O bonds for the other metals (or the Hg–O bonds with the nonrelativistic Hg pseudopotential). This is probably due to the much shallower potential curve for the less strongly bound mercury species.

Table 9 summarizes the water/metal chloride interaction energies for both $MCl_2 \cdot H_2O$ and $M_2Cl_2 \cdot H_2O$ complexes. The MP2 values are larger than the HF results by ca. 8–15 kJ mol^{-1} for the MCl_2 complexes but by ca. 16–20 kJ mol^{-1} for the M_2Cl_2 complexes. This suggests that dispersion type contributions to the interaction energies are slightly larger for the latter systems.[16a] The relativistic reduction of the interaction energy is larger for $HgCl_2 \cdot H_2O$ (ca. 31 kJ mol^{-1} at MP2) than for $Hg_2Cl_2 \cdot H_2O$ (ca. 21 kJ mol^{-1}). The interaction energies for $MCl_2 \cdot H_2O$ are somewhat larger than those for $M_2Cl_2 \cdot H_2O$ for M = Zn and Cd and for "nonrelativistic" M = Hg. However, relativity inverts this trend for M = Hg (i.e., the difference in the complexation energies of $Hg_2Cl_2 \cdot H_2O$ and $HgCl_2 \cdot H_2O$ is shifted ca. 10 kJ mol^{-1} by relativity).

While the energy differences between the complexation energies of M_2Cl_2 and MCl_2 are relatively small, it may be expected that for a more realistic number of solvent molecules the total effect will be larger. It is known that, e.g., the zinc and cadmium dichlorides are strongly dissociated in dilute aqueous solution whereas $HgCl_2$ is almost completely undissociated.[1-4,34] In fact, the group trends in the complexation energies for $MCl_2 \cdot H_2O$ (Table 9) agree excellently with calorimetric measurements for the group 12 dihalides in aqueous and DMSO solutions:[36] The heats of solvation for the zinc and cadmium dihalides are considerably larger than those for the mercury species. Our calculations clearly suggest that this is due to relativistic effects for the latter. We expect the differential relativistic effects in the solvation of Hg_2X_2 vs HgX_2 to be larger than suggested by the computational results for the simple monohydrate model systems. Hence, the influence of solvation probably shifts equilibrium 1 to the left for mercurous chloride but to the right for the corresponding zinc and cadmium species.

VIII. Influence of MX_2 and M_2X_2 Aggregation

A. Comparison of the Model Dimers $(MF_2)_2$ and $(M_2F_2)_2$ (M = Zn, Cd, Hg). We have chosen the dimers of M_2F_2 as simplest models for the aggregation of M_2X_2 species in the condensed phase. Their structures and the dimerization energies may be compared to the results of previous calculations for $(MF_2)_2$, at the same computational levels.[16] Figure 3 shows the results of HF/basis A optimizations for $(M_2F_2)_2$ within C_{2h} symmetry. Remarkably, all optimizations converged to symmetrically bridged D_{2h} dimers, even with M = Hg. The dimers $(MX_2)_2$ (X = F, Cl) also prefer D_{2h} structures for M = Zn and Cd[16b] (for M = Hg only at the nonrelativistic pseudopotential level[16a]). We have shown that relativistic effects reduce the interactions in $(HgX_2)_2$ (X = Hal) to such an extent that very unsymmetrically bridged structures with almost unperturbed linear HgX_2 monomeric units are found.[16a] Thus, structurally, $(Hg_2F_2)_2$ (Figure 3a) is in sharp contrast to $(HgF_2)_2$.[16a]

The bonding M–M distances and the terminal M–F distances for the dimers (Figure 3) are only very slightly (ca. 0.01 Å) longer than those for the monomers at the same computational levels (cf. Tables 1 and 2). In contrast, the bridging M–F bonds show the expected expansion by ca. 0.17–0.22 Å upon dimerization. While solid Hg_2F_2 exhibits parallel stacking of linear monomers[2] (cf. below), the Hg–F distance of ca. 2.16 Å is consistent with the HF value of ca. 2.23 Å for the dimer. Thus, the linear arrangement in the solid probably is dictated by the fact that each fluoride ion has to satisfy four next-nearest mercury neighbors.

As shown by the dimerization energies of HgF_2 and Hg_2F_2 (Table 10), the interactions for the former system are further reduced by relativity (by ca. 130 kJ mol^{-1} at MP2[16a]) than those for the latter (only by ca. 80 kJ mol^{-1}). In terms of structural and energetic consequences of dimerization, Hg_2F_2 is less different from Zn_2F_2 and Cd_2F_2 than HgF_2 is from ZnF_2 and CdF_2.

Table 11 investigates the addition of various contributions to the ANO–QCISD(T) energies for the gas-phase disproportion-

(36) See: Ahrland, S.; Kullberg, L.; Portanova, R. *Acta Chem. Scand., Ser. A* **1978**, *32*, 251 and references cited therein.

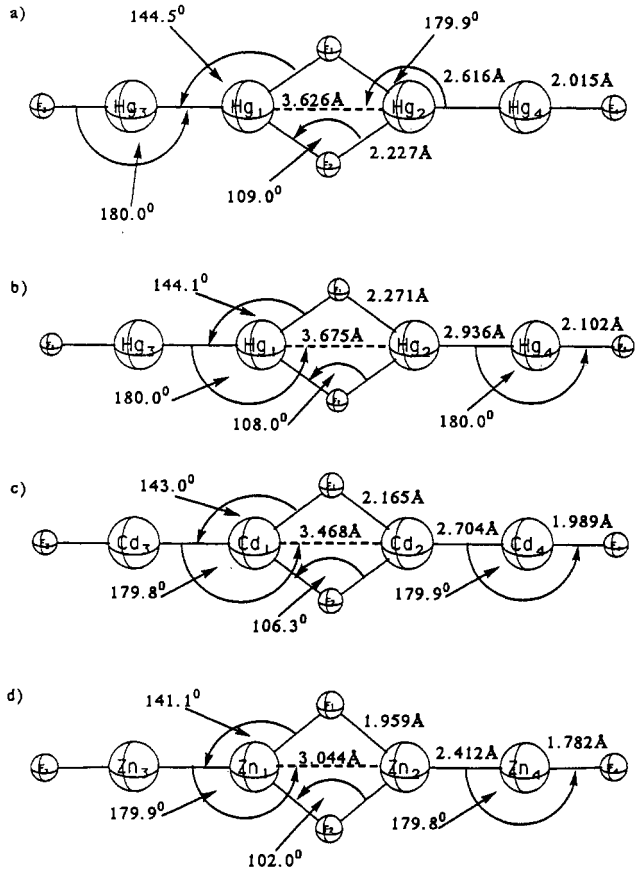

Figure 3. HF/basis A optimization results for $(M_2F_2)_2$ in C_{2h} symmetry: (a) M = Hg, quasirelativistic Hg pseudopotential; (b) M = Hg, nonrelativistic Hg pseudopotential; (c) M = Cd; (d) M = Zn.

Table 10. Comparison of MP2(HF)/Basis A Dimerization Energies for MF_2 and M_2F_2[a,b]

M	MF_2[b]	M_2F_2	M	MF_2[b]	M_2F_2
Zn	143.6 (177.8)	157.9 (170.8)	Hg_{nr}[c]	190.3 (207.6)	195.8 (200.1)
Cd	167.8 (184.6)	180.2 (183.3)	Hg_{rel}[d]	71.6 (79.9)	107.3 (116.2)

[a] MP2 calculations for $(M_2F_2)_2$ employ the HF structures whereas the MF_2 dimers and monomers have been fully MP2 optimized. [b] Data for MF_2 dimerization from ref 16. [c] Nonrelativistic Hg pseudopotential. [d] Quasirelativistic Hg pseudopotential.

Table 11. Contributions to Disproportionation Energies (kJ mol^{-1})

M	$M_2F_2(g) \rightarrow MF_2(g) + M(g)$[a]	$+H_{vap}(M)$[b]	$+H_{vap}(M) + E_{dim}$[c]
Zn	+36.7	-78.6	-64.3
Cd	+29.3	-70.6	-58.2
Hg_{rel}[d]	+7.1	-54.2	-18.5 (-24.2,[e] +63[f])

[a] ANO–QCISD(T) results; cf. Table 5. [b] Experimental heats of vaporization for the metals[3] added. [c] MP2/basis A dimerization energies for MF_2 and M_2F_2 (cf. Table 10) also added. [d] Quasirelativistic Hg pseudopotential. [e] Periodic Hartree–Fock energies of sublimation for HgF_2 and Hg_2F_2 added (cf. Table 15). [f] Experimental estimate for the reaction $Hg_2F_2(c) \rightarrow HgF_2(c) + Hg(l)$ (cf. ref 3).

ation (1) of M_2F_2: In the second column we add the experimental aggregation energies of the bulk metals. As discussed in section VI (cf. Table 6), this shifts the reaction energies to quite negative values. As a second step (third column in Table 11), we now add the MP2/basis A dimerization energies of MF_2 and M_2F_2 (cf. Table 10). While this does not change the situation much for M = Zn and Cd (except for a ca. 12–14 kJ mol^{-1} reduction of the exothermicity of the reaction), the equilibrium is shifted to the left by ca. 35 kJ mol^{-1} for M = Hg. Thus, the differential relativistic effects on the aggregation of the Hg^{I} and Hg^{II} halides contribute significantly to the stabilization of the former.

Table 12. Comparison of NPA Net Charges and Metal Valence Populations in HgF_2 and Hg_2F_2[a]

species	Q(M)	Q(F)	6s	6p	5d
HgF_2(rel)[b,c]	1.590	-0.795	0.568	0.024	9.982
HgF_2(nr)[b,d]	1.803	-0.901	0.227	0.020	9.946
Hg_2F_2(rel)[c]	0.877	-0.877	1.104	0.097	9.921
Hg_2F_2(nr)[d]	0.950	-0.950	0.960	0.113	9.977

[a] HF/basis A data. [b] Data for HgF_2 from ref 16a. [c] Nonrelativistic Hg pseudopotential. [d] Quasirelativistic Hg pseudopotential.

Table 13. ANO–QCISD(T) Ionization Energies (eV)

process	nr[a]	rel[b]	Δ_r[c]
$Hg_2 \rightarrow Hg_2^{2+} + 2e^-$	19.3	23.6	4.3
$2Hg \rightarrow 2Hg^+ + 2e^-$	16.5	20.4	3.9
$Hg \rightarrow Hg^{2+} + 2e^-$	23.7	28.7	5.0

[a] Nonrelativistic Hg pseudopotential. [b] Quasirelativistic Hg pseudopotential. [c] Relativistic contribution.

The electronic origin of the different relativistic influences on the dimerization of HgF_2 compared to Hg_2F_2 becomes clearer upon considering the atomic charges and metal valence populations computed for the monomers (Table 12; natural population analysis, NPA,[37] was employed). The formal oxidation states of Hg^{II} in HgF_2 and of Hg^{I} in Hg_2F_2 are roughly reproduced by the NPA charges, but as expected, the covalent bonding contributions to the Hg–F bond are larger for HgF_2 (cf. fluorine charges in Table 12). Relativity reduces the charge separation in the Hg–F bond in both cases. However, this reduction is less pronounced for the more ionic Hg–F bonds in Hg_2F_2.

Apparently, the presence of a Hg–Hg bond trans to the Hg–F bond allows more charge transfer in the latter, even when the relativistic increase in the Hg 6s-ionization energy is taken into account. These differences may be related to relativistic effects on the ionization energies of Hg_2 compared to Hg (Table 13): Due to the repulsion of the two positive charges, both the absolute value and the relativistic contributions to the energy of the formal reaction $Hg_2 \rightarrow Hg_2^{2+} + 2e^-$ are somewhat larger than those for the simultaneous monoionization of two separated mercury atoms. However, the double ionization of one mercury atom requires an even higher energy, and the relativistic contributions to this energy are ca. 0.7 eV larger. As the 6s electron of a mercury monocation is closer to the nucleus than in the neutral atom, the relativistic reduction of its kinetic energy is even larger. Therefore, the relativistic contribution to the second ionization energy is ca. 3 eV compared to ca. 2 eV for the first.[15] The extra energy needed to achieve the hypothetical situation $X^-Hg^{2+}X^-$ is ca. 5 eV but only ca. 4 eV for $X^-Hg_2^{2+}X^-$. In conclusion, the Hg–F bonds in Hg_2F_2 are more ionic than those in HgF_2, and the relativistic reduction of this ionicity is less in the former case. As a result, the interaction between two such bond dipoles in the dimers is considerably larger for $(Hg_2F_2)_2$ than for $(HgF_2)_2$, giving rise to a larger dimerization energy (Table 10).

B. Periodic Hartree–Fock Results for Crystalline Hg_2F_2 and HgF_2. To substantiate the transferability of the conclusions drawn above to the solid state, we compare crystal Hartree–Fock calculations on solid Hg_2F_2 and HgF_2. Detailed results for the latter compound are reported elsewhere.[16b] Relativistic effects are evaluated in the same manner as in the molecular calculations, i.e. by comparing results with quasirelativistic and nonrelativistic mercury pseudopotentials, respectively.

Table 14 compares calculated and experimental Hg_2F_2 structures. Comparison to molecular results at the same basis set level (cf. footnotes to Table 14) shows that the differences between quasirelativistic HF results and experiment are in the expected range. Obviously, relativity contracts the unit cell in the *c* direction, consistent with the reduction of bond lengths

(37) (a) Reed, A. E.; Weinhold, F. *J. Chem. Phys.* **1985**, *83*, 1736. (a) Reed, A. E.; Curtiss, L. A.; Weinhold, F. *Chem. Rev.* **1988**, *88*, 899.

Table 14. Comparison of Computed and Experimental Structural Parameters of Crystalline Hg_2F_2 (Lattice Constants and Bond Distances in Å)[a]

	nr[b]	rel[c]	exp[d]
a	3.543	3.643	3.673
c	12.221	11.118	10.884
z(Hg)	0.1188	0.1155	0.1152
z(F)	0.3108	0.3123	0.3143
Hg–Hg	2.899[e]	2.571[e]	2.508
Hg–F	2.345[e]	2.191[e]	2.157
Hg··F	2.652	2.699	2.711

[a] In space group *I*4/*mmm*. [b] Nonrelativistic Hg pseudopotential. [c] Quasirelativistic Hg pseudopotential. [d] Cf. ref 29. [e] At this basis set level, the quasirelativistic (nonrelativistic) distances in the monomeric Hg_2F_2 molecule are calculated as 2.549 (2.849) Å (Hg–Hg) and 2.003 (2.083) Å (Hg–F). Compare Table 1 for higher-level results.

Table 15. Comparison of Sublimation Energies (kJ mol^{-1}) for Hg_2F_2 and HgF_2

	nr[a,b]	rel[a,c]	exp
Hg_2F_2	211.2 (408.5)	168.7 (359.2)	
HgF_2[d]	298.5 (476.1)	138.7 (299.3)	128.9[e]

[a] Counterpoise-corrected results with uncorrected values in parentheses. [b] Nonrelativistic Hg pseudopotential. [c] Quasirelativistic Hg pseudopotential. [d] Cf. ref 16b. [e] Cf. ref 3.

within the Hg_2F_2 monomeric units. In contrast, the *a* and *b* lattice constants and Hg–F bonds to neighboring molecules are slightly increased by relativity.

The most interesting result, provided by a comparison of the sublimation energies of HgF_2 and Hg_2F_2, is shown in Table 15: The relativistic reduction of the sublimation energy of Hg_2F_2 is far less pronounced than that of HgF_2. Hence, while the sublimation energy of HgF_2 is considerably larger at the nonrelativistic level, that of Hg_2F_2 becomes larger at the quasirelativistic pseudopotential level. BSSE contributions to the aggregation energies are large, but they do not affect the general trend. The relativistic contributions are completely consistent with the above results for the HgX_2 dimers. Addition of these calculated sublimation energies to eq 1 shifts the equilibrium to the left by ca. 30 kJ mol^{-1} (cf. Table 11).

These considerations are supported by experimental energies for the solid-state equivalent of reaction 1:[38] From heats of formation for solid Hg_2X_2 and HgX_2 (X = F, Cl),[3] we calculate heats of ca. +63 kJ mol^{-1} (X = F) and ca. 35 kJ mol^{-1} (X = Cl) for the reaction $Hg_2X_2(c) \rightarrow HgX_2(c) + Hg(l)$. This should be compared to our best ANO–QCISD(T) energies (Table 5) of +7.1 kJ mol^{-1} (X = F) and −5.9 kJ mol^{-1} (X = Cl) for the gas-phase reaction. Thus, in spite of the aggregation energy of the metal, equilibrium 1 is shifted to the left by ca. 40–55 kJ mol^{-1} in the solid state for M = Hg (the accuracy of the experimental data is uncertain, due to appreciable decomposition of the fluorides at their sublimation temperatures; the reaction energies given might be too positive). This overcompensation of the metal aggregation by the differential aggregation contributions to the M^I and M^{II} halides may not be expected for M = Zn and Cd.

(38) While vaporization energies for MX_2 (X = Hal) are known for all group 12 metals, data for M_2X_2 are restricted to some mercury species (cf. ref 3).

IX. Conclusions

The gas-phase equilibrium $M_2X_2 \rightleftharpoons MX_2 + M$ provides no explanation for the larger condensed-phase stability of Hg_n^{2+} units compared to their Cd or Zn homologues. In fact, our high-level calculations strongly suggest that it should be easier to find Zn_2X_2 or Cd_2X_2 species in the gas phase than the corresponding Hg_2X_2. In spite of a moderate relativistic strengthening of the Hg–Hg bonds, equilibrium 1 is actually shifted to the right by relativity. Hence, condensed-phase interactions must be responsible for the wide occurrence of the Hg_2^{2+} cation.

Our ab initio calculations on suitable molecular model systems and on bulk Hg_2F_2 and HgF_2 indicate the following:

(a) The energies for the complexation of Hg_2X_2 (X = Hal) by solvent molecules are reduced less by relativity than those for HgX_2 complexation. As a result, solvation probably shifts equilibrium 1 to the right for M = Zn and Cd but to the left for M = Hg.

(b) Similarly, the aggregation energies for Hg_2X_2 (X = Hal) are reduced less by relativity than those for HgX_2. Thus, aggregation of the halide species shifts equilibrium 1 strongly to the left for M = Hg but probably only slightly so for M = Zn and Cd.

(c) The shift of equilibrium 1 to the right by contributions from the aggregation of the elemental metals is much less pronounced for M = Hg than for M = Zn and Cd (due to relativity[9,11]).

(d) The differential relativistic aggregation and solvation effects for the mercuric and mercurous halides are related to the influence of relativity on the charge separation in the Hg–X bonds.

Our results suggest that the stabilization of Zn_2^{2+} or Cd_2^{2+} in the condensed phase is only possible in systems where the aggregation or solvation of the M^{II} species is considerably less favorable than that of the $(M^I)_2$ compounds. Additionally, for obvious reasons, the electronegativity of the substituents has to be large. In analogy to the use of dithianes or selenadithianes in mercury(I) chemistry,[2] one might envision complexes of sterically hindered amines or ethers to stabilize the Cd_2^{2+} or Zn_2^{2+} ion.

Recently, we showed that the existence of oxidation state IV seems possible for mercury but not for zinc or cadmium, due to the relativistic destabilization of bonds between Hg^{II} and electronegative ligands like fluorine.[15] It is interesting to note that the stability of mercury(I) may also be traced back to a relativistic reduction of (in this case intermolecular) interactions for the mercury(II) competitors (and of those for bulk mercury). Thus, mercury has better access to oxidation states different from +II than zinc or cadmium, due to the influence of relativity.